ETH zürich

Effects of inter-crystal optical separation layers on unwanted light crosstalk and on performance parameters of the SAFIR PET/MR scanner

Pascal L. Bebié, Institute for Particle Physics and Astrophysics, Department of Physics, ETH Zurich

SAFIR

Introduction: Positron Emission Tomography (PET)

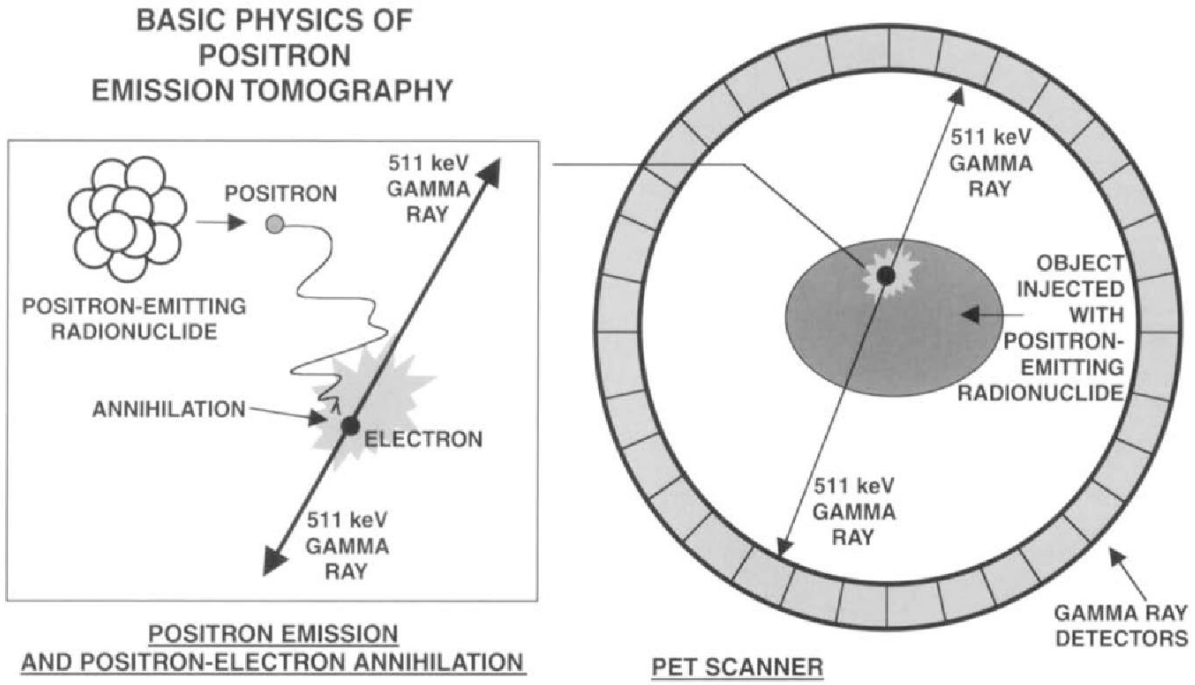

- Injection of radioactive tracer (molecule or process under study)
- Metabolism transports tracer; accumulation
- Annihilation: clear signature
- Identification of signature: energy and timing
- A problem: Compton scattering, scattering to neighbouring detector elements (loss of spatial resolution / coincidence rate)

Figure: S. Cherry, et al., DOI:10.1093/ILAR.42.3.219

Introduction: The SAFIR Project

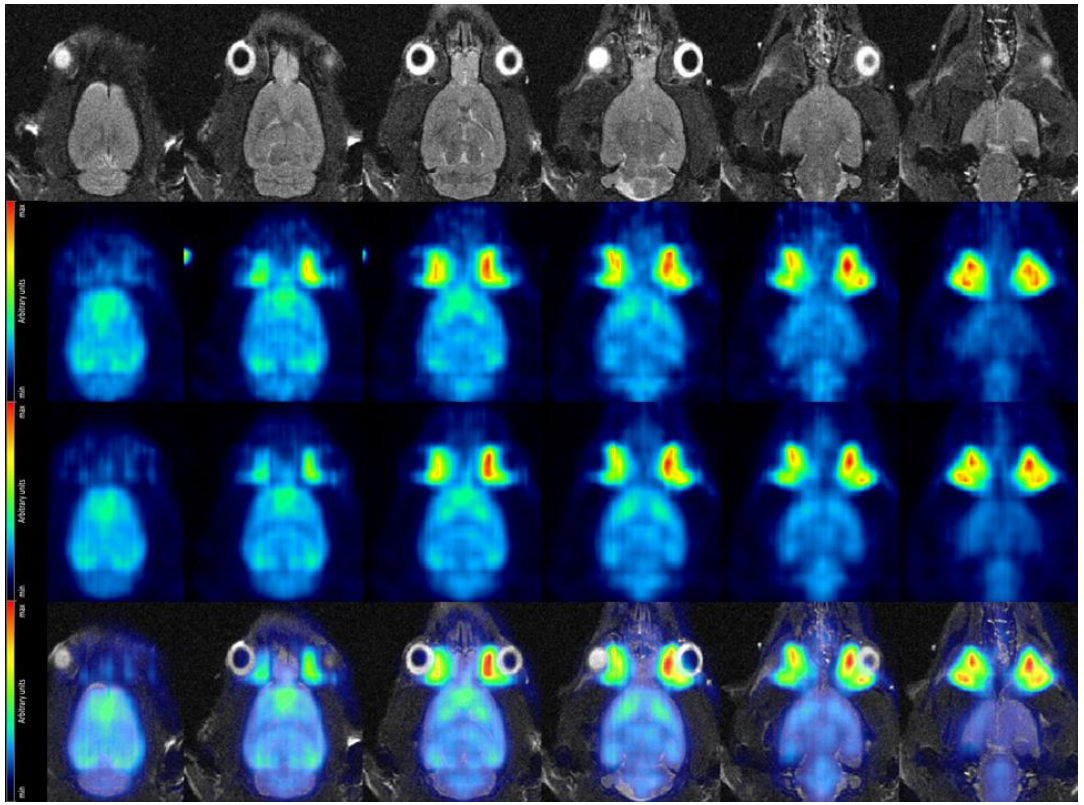

Figure: P. Bebié, et al., https://doi.org/10.3390/s21217037

- SAFIR: PET insert to a 7T Bruker BioSpec 70/30 USR MRI (structural & functional imaging)
- Construction to needs of pharmacologists (B. Weber group and others)
- High injected activity (ca. 500MBq) → high coincidence rate / high count statistics in short times → fast image formation / high temporal resolution
- Observation of fast kinetics of molecular readouts
- Requirement of best possible energy & timing resolution, average spatial resolution
- Requirement for minimal pile-up and dead-time

Introduction: SAFIR-I

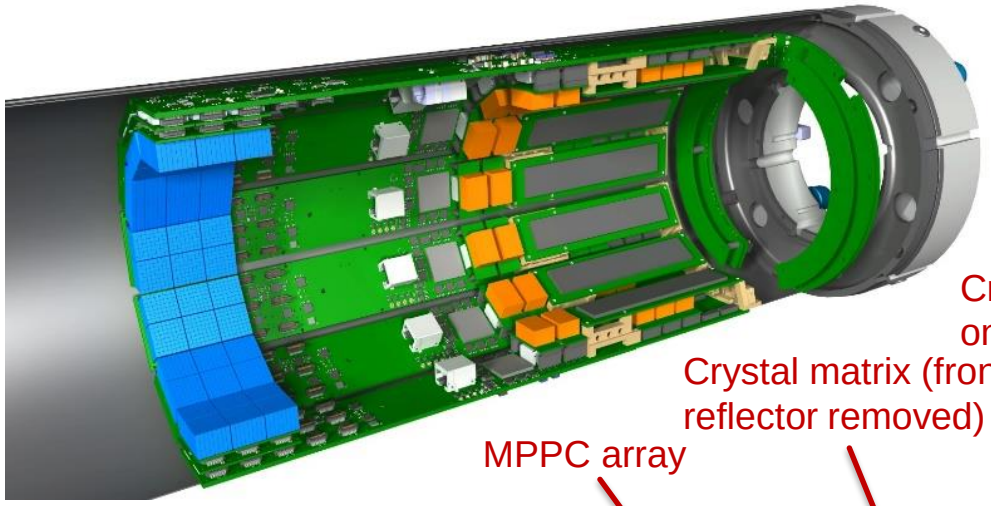

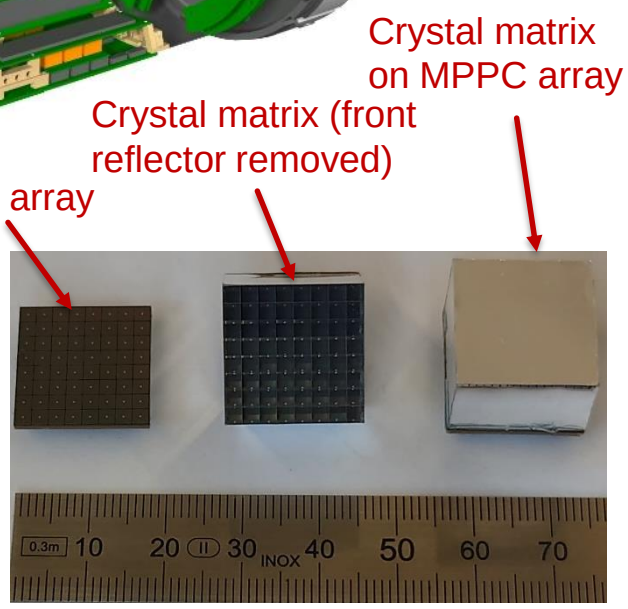

- SAFIR-I evolved from previous prototype design [1].
- LYSO crystals (Sichuan Tianle Photonics) separated by bonded 3M Enhanced Specular Reflector (ESR) films.
- Optical adhesives known to reduce reflectivity of ESR films [2].
- 8×8 crystal matrices, 1-to-1 coupled to SiPMs
- Readout: Hamamatsu TVS MPPC 13361-2050 SiPM arrays, 2.2mm pitch
- Off-line analysis
- Coincidence windows: 500ps, 391-601keV

[1] C. Ritzer, et al. “Initial Characterization of the SAFIR Prototype PET-MR Scanner,” *IEEE Trans. Radiat. Plasma Med. Sci.,* vol. 4, no. 5, pp. 613-621, Sept. 2020.
[2] F. Loignon-Houle, C. Pepin, S. Charlebois, R. Lecomte, “Reflectivity quenching of ESR multilayer polymer film reflector in optically bonded scintillator arrays,” *Nucl. Instrum. Methods Phys. Res. A,* vol. 851, pp. 62-67, Apr. 2017.

Materials

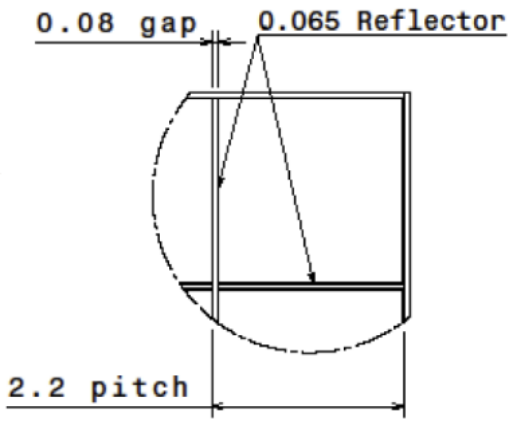

Type A [baseline]

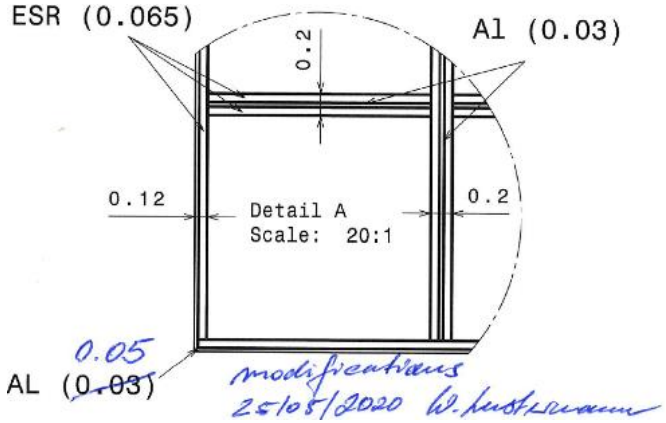

Type B

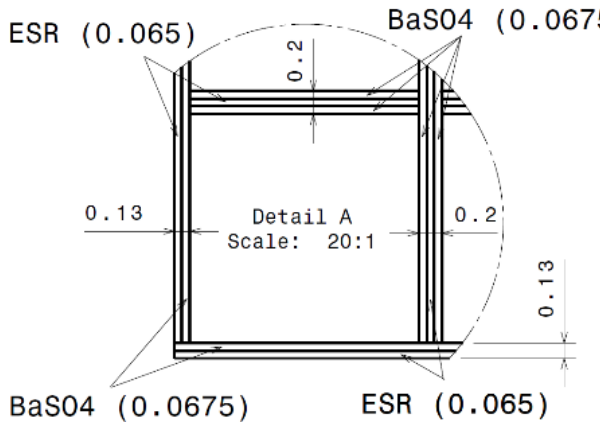

Type C

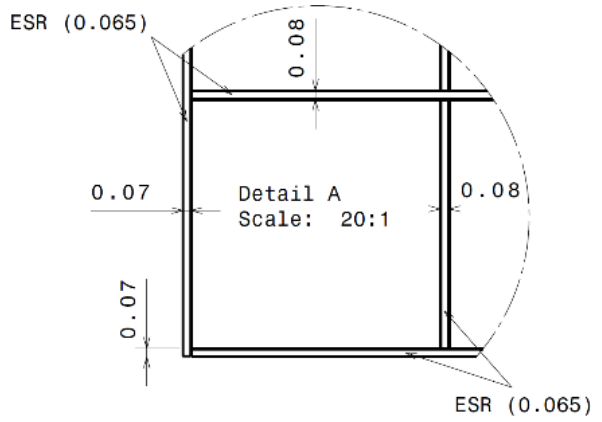

Type D

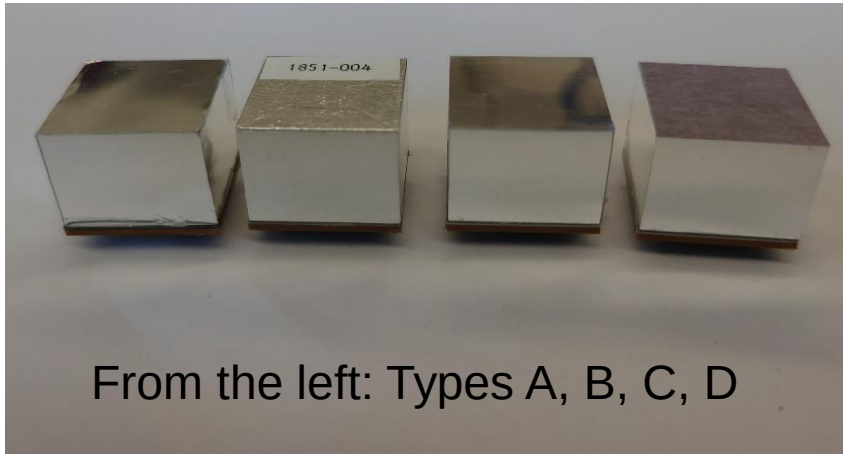

From the left: Types A, B, C, D

Crystal size for types A & D was 2.1mm × 2.1mm × 13.0mm, for types B & C it was 2.0mm × 2.0mm × 13.0mm

Methods

All measurements: Noise hits <7.5keV rejected by PETA6SE [3] ASIC

Low activity measurements (^{18}F, <10MBq, point-like source):

- Pre-measurements to determine event definition
- *Event* definition: One *primary hit* with 391keV<E<601keV in one of the four central crystals of the 8×8 matrix, plus all hits registered -3ns to +6ns from arrival of primary hit, E<300keV.
- Ca. 430k events per matrix; four matrices tested per type
- Observations for central 4 crystals of each matrix (3 full “neighbour-squares” of crystal elements around each)
- Results systematically averaged over same-type matrices
- Estimated background noise is subtracted (avg. of values at least 5 crystals away)

[3] Sacco, C. Chang, M. Ritzert, P. Fischer, C. Levin, "An integrated circuit readout for tof-pet detectors for pet/mri (conference presentation)," Radiation Detectors in Medicine Industry and National Security XVIII, vol. 10393, pp. 103930V, 2017.

Methods

All measurements: Noise hits <7.5keV rejected by PETA6SE [3] ASIC

High activity coincidence measurement inside SAFIR-I:

- ^{18}F, 546MBq line source (75mm long, 4.5mm diameter)
- Ideal readout parameters of ASIC for each matrix type determined in pre-meas. (noise level)
- Compare coincidence resolving time (CRT), energy resolution and coincidence rate
- 125mm distance between crystal front faces
- Estimated coincidence detection efficiency reduction for B & C due to smaller crystal size: 15.3% (solid angle considerations)

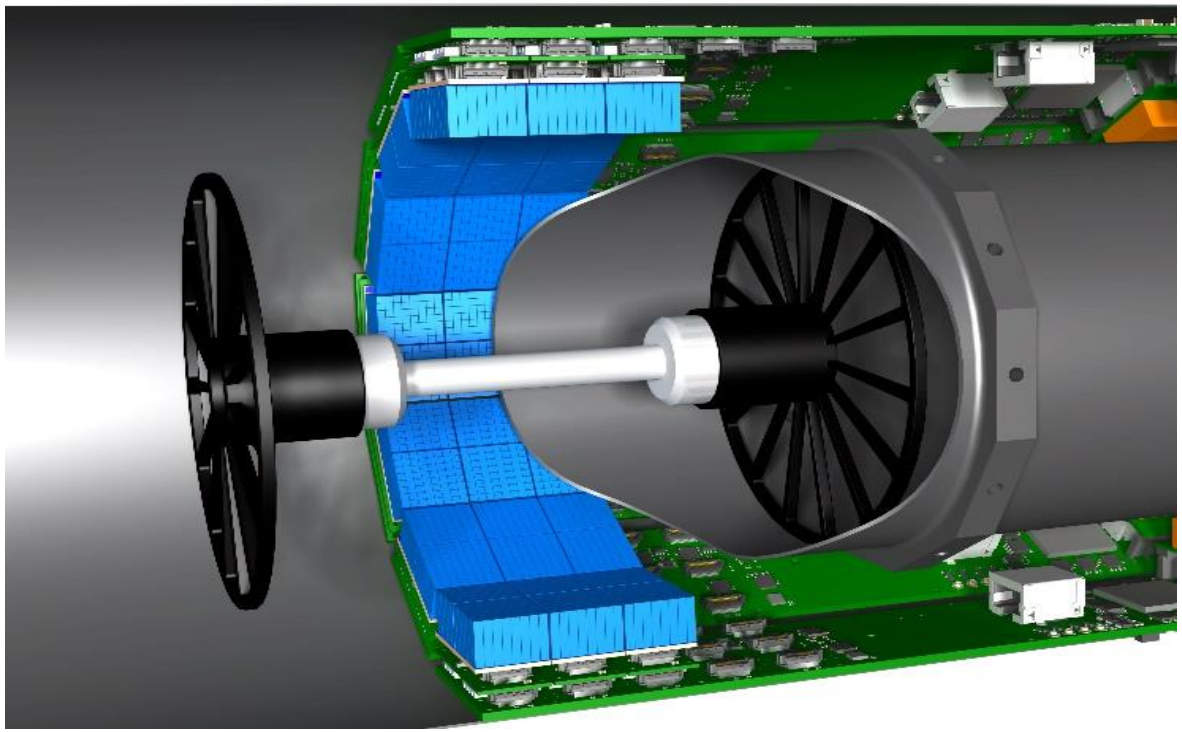

[3] Sacco, C. Chang, M. Ritzert, P. Fischer, C. Levin, "An integrated circuit readout for tof-pet detectors for pet/mri (conference presentation)," Radiation Detectors in Medicine Industry and National Security XVIII, vol. 10393, pp. 103930V, 2017.

Results

Low rate results:

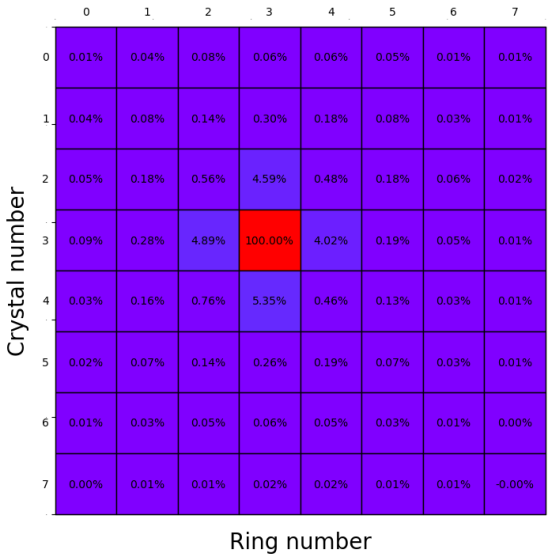

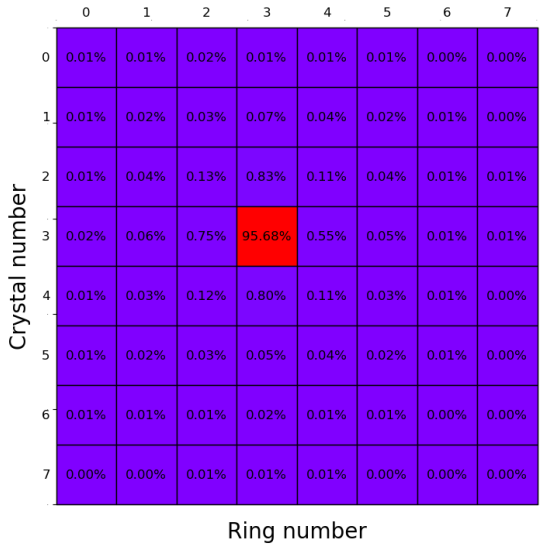

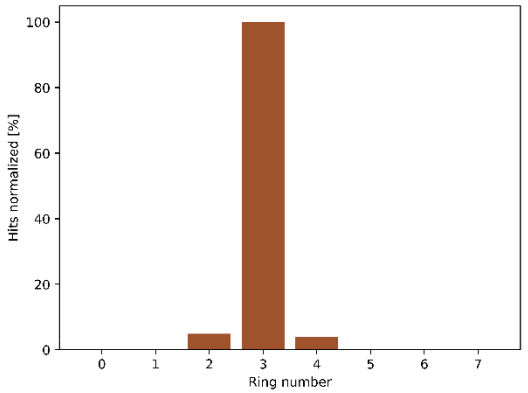

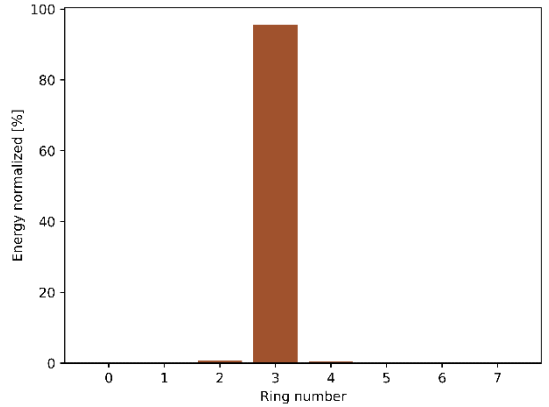

Example: Type A matrix; left side: Pos. 3-3 (primary hit) counts and energy, right side: profile crystal no. 3

Optical crosstalk was observed for all types, primarily to directly neighboring crystals sharing a side face, secondarily to diagonal neighbors sharing a crystal edge.

Results

Low rate results:

Matrix Type	Avg. energy in primary hit [%]	Avg. number of hits per event
A(*)	95.1 ± 0.8	1.41 ± 0.12
B	97.7 ± 0.4	1.13 ± 0.02
C	92.5 ± 0.5	2.28 ± 0.11
D	96.2 ± 0.3	1.38 ± 0.03

(*) one outlier (>2σ) removed form analysis

A: ESR-glue-ESR / B: ESR-Aluminium-ESR / C: ESR-$BaSO_4$-ESR / D: Single-layer ESR (no glue)

Results

High rate results:

Matrix Type	CRT [ps]	Energy resolution [%]	Coinc. det. rates relative to A (solid angle estimate) [%]
A	290 ± 7	18.9 ± 0.3	100 (100)
B	228 ± 5	14.3 ± 0.2	90 (84.7)
C	280 ± 5	17.3 ± 0.3	81 (84.7)
D	332 ± 4	15.6 ± 0.2	107 (100)

A: ESR-glue-ESR / B: ESR-Aluminium-ESR / C: ESR-$BaSO_4$-ESR / D: Single-layer ESR (no glue)

Discussion I

- Optical crosstalk for current-design inter-crystal separation layer (type A) confirmed.
- Minimization of optical crosstalk by appropriate separation layer choice possible.
- Type D shows less crosstalk than type A; while the results are still within large errors compatible at low rate, this becomes evident at high rate. The high rate measurement appears to be more sensitive to differences between the types.
- Comparison between types A & D confirms finding by F. Loignon-Houle et al.[2] that the surrounding glue increases ESR film transparency.

[2] F. Loignon-Houle, C. Pepin, S. Charlebois, R. Lecomte, “Reflectivity quenching of ESR multilayer polymer film reflector in optically bonded scintillator arrays,” *Nucl. Instrum. Methods Phys. Res. A,* vol. 851, pp. 62-67, Apr. 2017.

Discussion I (cont.)

- The smaller crystal size of types B & C leads to a reduced coincidence detection efficiency compared to type A. Type D has the highest coincidence detection efficiency due to identical crystal size but reduced crosstalk compared to type A.
- For types B & D, reduced crosstalk (hence lower PETA ASIC dead time) in comparison with type A facilitates activity-dependent coincidence detection rate improvement. Such improvements could in principle also be achieved using longer acquisition times or higher activities.
- Type B shows cleanest events at low rate and best CRT and energy resolution at high rate.
- Bonus: Type B performance observed to be less dependent on ASIC noise threshold; matrix can be employed with lower threshold for larger activty range of optimal performance
- Effect of bringing additional metal into the MRI?

Assessment of MR compatibility of aluminium between crystals

- Total amount of alu between crystals (SAFIR-II, 8 detector ring blocks): 2.3e-5 m^3
- Amount of alu in the form of heatsinks in SAFIR-I (3 d.r. blocks): 2.0e-5 m^3 [SAFE]
- Amount of alu originally planned to be used in the form of heatsinks on the PETA chips: 5.4e-5 m^3
- Built mock-up with alu plates
- Vertical orientation of alu layers between crystals explicitly considered
- Lattice structure of alu between crystals explicitly considered with orthogonal plates
- Different distance to bore/coil compared to heat sinks explicitly considered in new model
- Total amount of alu in model: 2.4e-5 (~4% more; for symmetry reasons)
- Bruker: Dedicated water phantom and MR sequences to test compatibility

Assessment of MR compatibility of aluminium between crystals

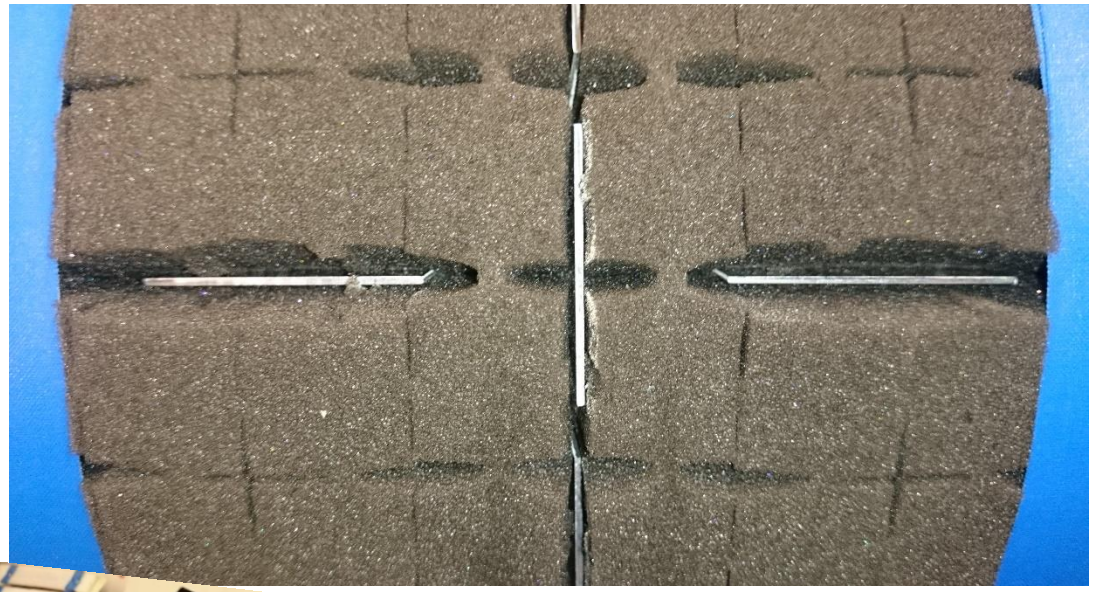

Results & Discussion II

MR compatibility of alu. vs SAFIR-I with type A matrices (average of 5 meas. for each line)

MRI SNR [1/mm^3] alu. mock-up

- Baseline: 2539 +/- 10
- Off: 2602 +/- 19 (+2.5% vs. baseline)

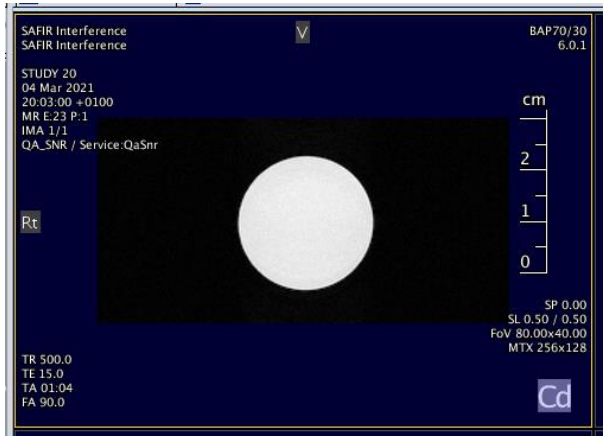

MRI SNR [1/mm^3] SAFIR-I

- Baseline: 2532 +/- 6
- Off: 2622 +/- 8 (+3.6% vs. baseline)

→ No SNR degradation, no artifacts in MR image

→ Type B matrices can safely be used

Contact information and credits

ETH Zurich
Pascal L. Bebié
Department of Physics, Institute for Particle Physics and Astrophysics
Otto-Stern-Weg 5
CH-8093 Zurich
E-Mail: bebiep@phys.ethz.ch

https://dissertori-group.ethz.ch/research/detector-rd-and-applications-in-biomedical-imaging/safir.html

Design: Pascal L. Bebié
Images: SAFIR collaboration
Acknowledgment: Special thanks to R. Wixinger for preparing the low rate analysis software and collaborating on the pre-studies and to C. Ritzer for adapting the coincidence analysis software.